Journal of Power Sources 195 (2010) 7466–7470

Contents lists available at ScienceDirect

Journal of Power Sources

journal homepage: www.elsevier.com/locate/jpowsour

Short communication

Sodium-ion transfer at the interface between ceramic and organic electrolytes

Fumihiro Sagane, Takeshi Abe*, Zempachi Ogumi

Graduate School of Engineering, Kyoto University, Nishikyo-ku, Kyoto 615-8510, Japan

ARTICLE INFO

Article history:
Received 8 April 2010
Received in revised form 14 April 2010
Accepted 16 April 2010
Available online 12 May 2010

Keywords:
Sodium-ion transfer
Sodium-ion batteries
Interface
Ceramic electrolyte

ABSTRACT

Sodium-ion transfer through the interface between ceramic and organic electrolytes was studied by AC impedance spectroscopy. $Na_3Zr_{1.88}Y_{0.12}Si_2PO_{12}$ (NASICON) and Na-β″-alumina were used as ceramic electrolytes, and propylene carbonate (PC) and dimethyl sulfoxide (DMSO) containing 0.05 mol dm^{-3} $NaCF_3SO_3$ were used as organic electrolytes. The semi-circle ascribed to interfacial charge transfer resistance (R_{ct}) was observed. The activation energies for sodium-ion transfer at the interface between ceramic and organic electrolytes were evaluated by the temperature dependency of R_{ct}. As a result, the activation energies depended on the ceramic electrolytes but not on the solvents. These results suggest that sodium-ion transfer from ceramic to organic electrolytes should be responsible for the activation energies, which is contrary to the case in a lithium-ion transfer system. Based on these results, the mechanism of interfacial sodium-ion transfer was discussed.

1. Introduction

One of the major driving forces behind recent R&D on lithium-ion batteries (LIB) is the development of advanced-transportation systems, such as plug-in hybrid electric vehicles (PHEVs) and electric vehicles (EVs). These applications demand that lithium-ion batteries meet some strict requirements: high safety, long cycle lives, high energy densities, high rate performance, etc. In addition, sources for lithium and other elements used in LIB should also be considered if the above EVs become popular.

Since sodium is more abundant than lithium, sodium-ion batteries are candidates as new battery systems. Sodium-ion batteries require host materials for sodium-ion insertion and extraction. Carbons and some oxides have been studied as negative and positive electrodes for use in sodium-ion batteries [1–9].

Sodium-ion batteries should exhibit fast sodium-ion kinetics at the electrodes. We have previously focused on the kinetic aspects of charge–discharge reactions in lithium-ion batteries to enhance their rate capabilities [10–13]. In these studies, we found that large activation barriers exist at the interface between electrodes and electrolyte and that the Lewis basicities of the solvents are responsible for the large activation energies. For a lithium-ion transfer system, the interactions between lithium-ion and solvent in the electrolyte play a dominant role in determining the activation energies. Sodium-ion is less Lewis-acidic than lithium-ion and therefore we can expect fast sodium-ion transfer at the interface between the electrode and electrolyte in sodium-ion batteries.

To elucidate the above hypothesis, we focused on sodium-ion transfer at the interface between electrode and electrolyte. To shed light on only sodium-ion transfer, we fabricated a model interface consisting of sodium-ion conductive ceramic and organic electrolytes. We describe here studies on sodium-ion transfer at the interface between ceramic and organic electrolytes by AC impedance spectroscopy.

2. Experimental

2.1. Sample preparation

For sodium-ion conductive ceramics, $Na_3Zr_{1.88}Y_{0.12}Si_2PO_{12}$ (NASICON) and Na-β″-alumina were used. NASICON was prepared by a solid-state reaction as reported by Fuentes et al. [14] Powders of $Na_3PO_4{\cdot}12H_2O$, ZrO_2, SiO_2 and Y_2O_3 were mixed in a planetary ball mill and then calcined at 1100 °C. After being mixed and calcined again, the powder was pressed into a pellet, which was sintered at 1230 °C. The sample was characterized by X-ray diffraction (XRD) (Rint 2200, Rigaku). Na-β″-alumina was purchased from Ionotec, Ltd. Sodium-ion conductivities for these ceramics were measured by an AC impedance method within a frequency range from 1 MHz to 1 Hz using a cell of SUS (stainless steel)/solid electrolyte/SUS. To achieve good contact between SUS and the ceramic electrolyte, gold metal was sputtered onto these solid electrolyte pellets. Liquid electrolytes were propylene carbonate (PC) or dimethyl sulfoxide (DMSO) containing 0.05 mol dm^{-3} $NaCF_3SO_3$. PC, DMSO (Kishida Chemical Co.), and $NaCF_3SO_3$ (Aldrich) were used without further purification.

* Corresponding author. Tel.: +81 75 383 2487; fax: +81 75 383 2488.
E-mail address: abe@elech.kuic.kyoto-u.ac.jp (T. Abe).

0378-7753/$ – see front matter © 2010 Elsevier B.V. All rights reserved.
doi:10.1016/j.jpowsour.2010.04.054

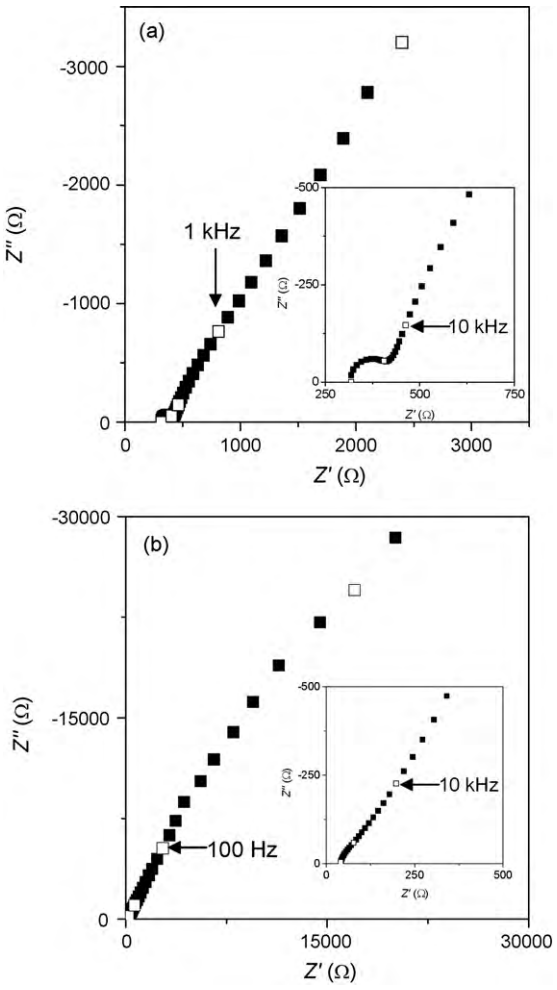

Fig. 1. Complex impedance plots for (a) Au/NASICON/Au and (b) Au/β″-alumina/Au. Insets are the magnified plots in the higher frequency region.

2.2. Electrochemical measurements for interfacial sodium-ion transfer

For electrochemical measurements, a symmetric four-electrode cell consisting of counter electrode/organic solution/solid electrolyte/organic solution/counter electrode was fabricated. Reference electrodes were inserted in each solution. Counter and reference electrodes were Pt or Ag wires. The interfacial area was maintained at 0.20 cm^2 geometrically. Four-electrode electrochemical impedance measurements were conducted with a Solartron 1260 & 1287 within a frequency range from 1 MHz to 100 mHz. The impedance spectra were analyzed using a non-linear least-squares fitting program (Z view 2). All experiments were conducted under an Ar atmosphere. The details of the experiments have been described previously [15].

3. Results and discussion

3.1. Bulk properties of solid electrolyte

The XRD pattern (not shown) was in good agreement with that in the literature [14], although a small amount of monoclinic ZrO_2 was observed.

A complex impedance plane plot for a cell of Au/NASICON/Au at 280 K is shown in Fig. 1(a). One semi-circle was seen in the high-frequency region due to grain boundary resistance, and this was followed by the appearance of blocking-electrode behavior. A semi-circle ascribed to the bulk resistance was not observed within the present frequency regions. Note that the characteristic frequencies of both the bulk and grain boundary resistances are over 100 kHz. This value is very important for understanding the impedance spectra given below. It was difficult to accurately determine the values of the bulk and grain boundary resistances, since the semi-circle observed was somewhat depressed due to inductance. The sodium-ion conductivity evaluated from the total value of these resistances was 1.3×10^{-3} S cm^{-1} (at room temperature), and the activation energy was calculated to be 30 kJ mol^{-1}. These values are in good agreement with the previous report [15].

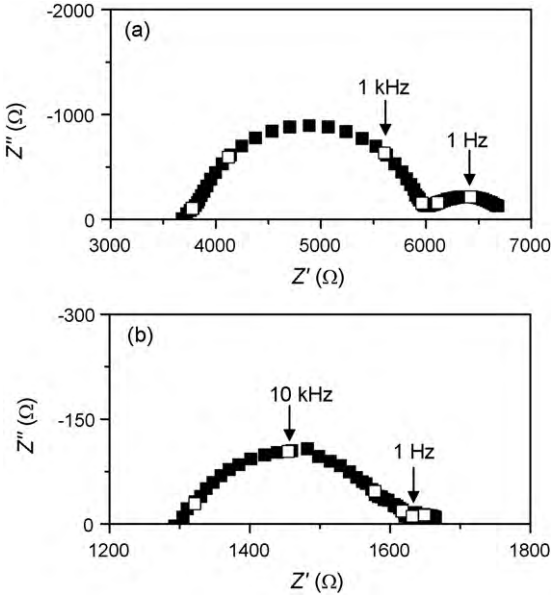

Fig. 2. Complex impedance plots for Pt/$NaCF_3SO_3$–DMSO/NASICON/$NaCF_3SO_3$–DMSO/Pt (four-electrode cell, 303 K). The $NaCF_3SO_3$ concentration was (a) 0.05 mol dm^{-3} and (b) 0.4 mol dm^{-3}.

Fig. 1(b) shows a complex impedance plot for a cell of Au/β″-alumina/Au at 303 K. A semi-circle corresponding to the grain boundary resistance was observed in the high-frequency region, and most of the spectrum showed blocking-electrode-type behavior. Again, the characteristic frequency for grain boundary resistance was over 100 kHz. The total conductivity of the sample at room temperature was 7.2×10^{-4} S cm^{-1}, which was consistent with that reported by Ionotec, Ltd. [16].

3.2. Sodium-ion transfer at the interface between ceramic and organic electrolytes

A complex impedance plot for a cell of Pt/0.05 mol dm^{-3} $NaCF_3SO_3$–DMSO/NASICON/0.05 mol dm^{-3} $NaCF_3SO_3$–DMSO/Pt at 303 K (4-electrode measurement) is shown in Fig. 2(a). Two semi-circles were observed with characteristic frequencies of about 3 kHz and 1 Hz. The symmetric cell should give the following impedance as (*i*) the bulk resistance of DMSO-based electrolyte, (*ii*) the bulk and grain boundary resistances of NASICON, and (*iii*) the charge transfer resistance at the NASICON/DMSO-based electrolyte interface. Interfacial resistance between the counter electrode and organic electrolyte is not observed due to the four-electrode measurements. Among these resistances, ion diffusion in DMSO-based electrolyte and in NASICON bulk is so fast that these resistances would not give semi-circles in the present frequency regions. The impedance of grain boundary resistance with a characteristic frequency exceeding 100 kHz should appear as a shoulder above a frequency of 100 kHz. Based on the above discussion, the impedance spectrum for the symmetrical cell

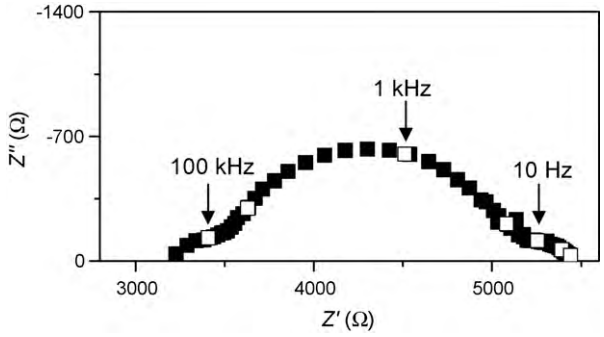

Fig. 3. Complex impedance plot for $Pt/NaCF_3SO_3$–DMSO/Na-β″-alumina/$NaCF_3SO_3$–DMSO/Pt (four-electrode cell, 303 K).

should give only one semi-circle due to the sodium-ion transfer at the NASICON/DMSO-based electrolyte interface. However, we observed two semi-circles, as shown in Fig. 2(a). The semi-circle in the lower frequency region is quite depressed and sometimes seemed to disappear due to the small resistances. In contrast, the semi-circle in the higher frequency region is clearly observed in every measurement.

To elucidate these relaxation processes, the dependence of the impedance components on the sodium-ion concentration was studied. Fig. 2(b) shows the complex impedance plot for a cell of $Pt/0.4\,mol\,dm^{-3}$ $NaCF_3SO_3$–DMSO/NASICON/$0.4\,mol\,dm^{-3}$ $NaCF_3SO_3$–DMSO/Pt at 303 K. Again, two semi-circles with characteristic frequencies of about 10 kHz and 1 Hz were seen. As is clear in Fig. 2(a) and (b), the two impedance components decreased with an increase in the salt concentration. This means that these semi-circles are associated with the relaxation process of ion transfer. As mentioned above, the semi-circle in the lower frequency region seemed to disappear in some cases. NASICON ceramic electrolyte was sintered. However, when sintering is not sufficient, micropores and mesopores should exist in NASICON ceramic electrolyte. We assume that the semi-circle in the lower frequency region can be ascribed to the sodium-ion and anion transfer processes through these pores. In fact, a four-probe cell of Li/lithium-ion conductive liquid electrolyte/porous electrode/lithium-ion conductive liquid electrolyte/Li was fabricated by using two reference electrodes of Li. We tried to evaluate ion diffusion through the porous electrode by AC impedance spectroscopy. As a result, we observed a semi-circle due to ion conduction in the porous electrode. Therefore, the other semi-circle in the higher frequency region in Fig. 2 should be ascribed to the sodium-ion transfer process.

Fig. 3 shows a complex impedance plot for a cell of $Pt/0.05\,mol\,dm^{-3}$ $NaCF_3SO_3$–DMSO/β″-alumina/$0.05\,mol\,dm^{-3}$ $NaCF_3SO_3$–DMSO/Pt. Three semi-circles with characteristic frequencies of about 100 kHz, 1 kHz, and 10 Hz were observed. The semi-circles could be assigned based on a comparison to the plot in Fig. 1(b) and the dependence of the impedance plot on the concentration of electrolyte salts; the semi-circle in the high-frequency region was ascribed to the grain boundary resistance of Na-β″-alumina. Based on a similar consideration, the semi-circles in the mid- and low-frequency regions were ascribed to the sodium-ion transfer resistance and ion conduction resistance in the pores, respectively.

Fig. 4 shows the temperature dependence of sodium-ion transfer resistances at the interfaces between NASICON and organic electrolytes and between β″-alumina and organic electrolytes. Arrhenius-type behavior was observed for all plots and the activation energies for sodium-ion transfers were calculated from their slopes. Table 1 shows the values of the activation energies. As is clear from Table 1, the activation energies are almost the same regardless of the solvent in the electrolyte. However, the activation energies varied according to the ceramic electrolytes. Since DMSO is a stronger Lewis base than PC based on a consideration of Gutmann's donor number (15.1 for PC and 29.8 for DMSO [17]), the interaction between sodium-ion and DMSO must be greater than that between sodium-ion and PC. In our previous work, we evaluated the activation energies for lithium-ion transfer at the interface between a lithium-ion conductive electrolyte of $La_{0.55}Li_{0.35}TiO_3$ and organic electrolytes [12]. In the case of a lithium-ion transfer system, the activation energies depended on the solvents in the electrolyte and, based on the calculated interaction between lithium-ion and solvent, we could conclude that the Lewis basicities of the solvents are responsible for the activation energies. When the sodium-ion transfer system is similar to that for lithium-ion transfer, the activation energy for sodium-ion transfer at a NASICON/DMSO-based electrolyte should be higher than that for a NASICON/PC-based electrolyte. However, the activation energies are almost the same when the ceramic electrolyte is the same.

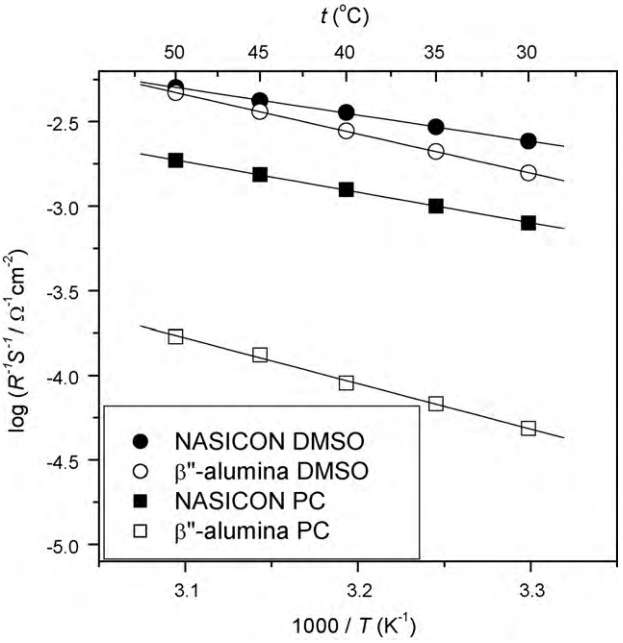

Fig. 4. Temperature dependency for the solid/liquid interfacial resistances.

The activation energies are determined by the difference in the chemical potential of sodium-ion in the ceramic electrolyte and the transition state or by the difference in the chemical potential of sodium-ion in the electrolyte and the transition state. The present results can be explained by the schematic shown in Fig. 5. When we assume that the chemical potentials of sodium-ion in ceramic electrolytes are lower than those in liquid electrolytes, we can explain the activation energies in the present work.

The activation energies varied slightly according to whether DMSO or PC was used as a solvent, which may be ascribed to the difference in the transition states, as shown in Fig. 5. In this discussion, the transition state is assumed to be the same regardless of the ceramic electrolytes. To clarify this assumption, sodium-ion transfer at the interface between the ceramic and polymer electrolytes was investigated. The interaction between sodium-ion and polymer electrolyte is generally so strong that the chemical potential of

Table 1
Activation energy for interfacial sodium-ion transfer.

	PC	DMSO
NASICON	$35\,kJ\,mol^{-1}$	$30\,kJ\,mol^{-1}$
β″-Alumina	$52\,kJ\,mol^{-1}$	$45\,kJ\,mol^{-1}$

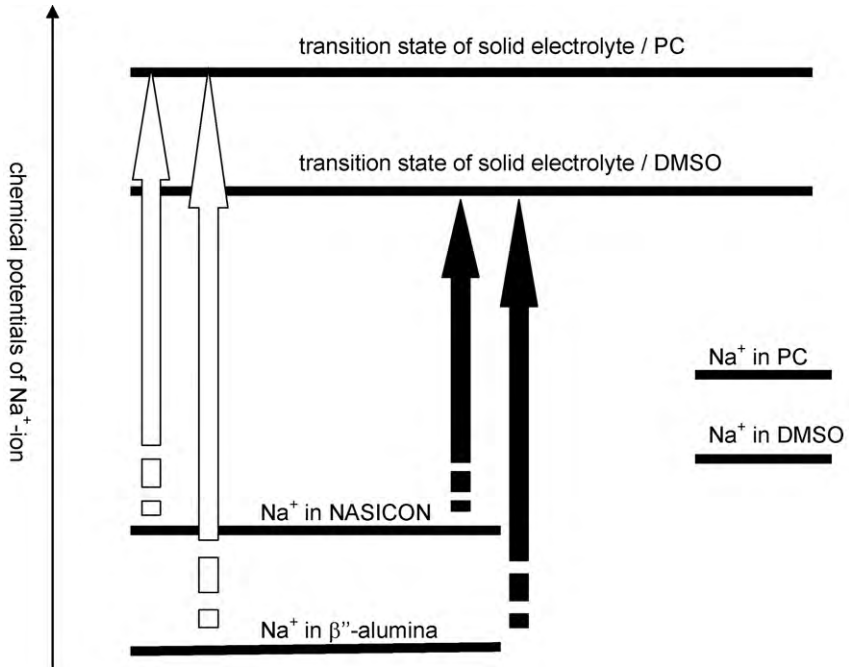

Fig. 5. Schematic of energy diagram for sodium-ion transfer at interface between ceramic and organic electrolytes.

sodium-ion in a polymer electrolyte must be lower than that in a ceramic electrolyte. Thus, the de-solvation process of sodium-ion from the polymer electrolyte will be rate-determining.

A two-electrode cell consisting of SUS/polymer/solid electrolyte/polymer/SUS was fabricated and AC impedance measurements were performed. For the polymer electrolyte, $NaCF_3SO_3$–poly (ethylene oxide) (PEO) was used. The details of the experimental conditions have been described previously [15].

Fig. 6 shows the temperature dependence of the interfacial resistances for sodium-ion transfer between ceramic and polymer electrolytes. The activation energies of ca. 70 kJ mol^{-1} were much higher than those for sodium-ion transfer at the interface between ceramic and organic electrolytes, which indicates that the sodium-ion transfer process from polymer electrolyte to ceramic electrolyte was rate-determining. Since the activation energies of 70 and 72 kJ mol^{-1} are almost the same, we can conclude that the transition state should be at almost the same level regardless of the ceramic electrolytes used.

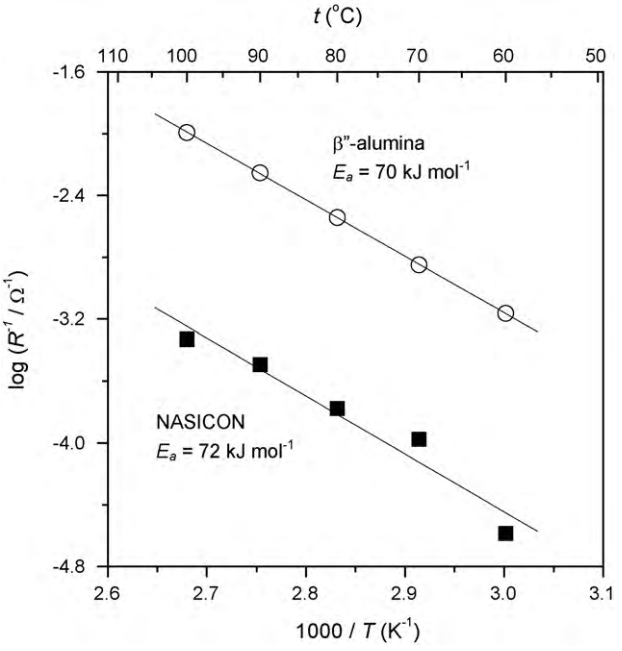

Fig. 6. Temperature dependency of the solid electrolyte/PEO interfacial resistances.

4. Conclusions

Sodium-ion transfer at the interface between ceramic and organic electrolytes was studied by AC impedance spectroscopy. We clarified the mechanism of sodium-ion transfer at the interface between a ceramic and organic electrolyte. Sodium-ion transfer from a ceramic electrolyte to an organic electrolyte has a greater activation barrier than that from an organic to ceramic electrolyte. Also, when the ceramic electrolyte is NASICON, the activation energy for sodium-ion transfer is ca. 30 kJ mol^{-1}, which is much smaller than that for the lithium-ion transfer system. This result indicates that the sodium-ion kinetics at electrodes for sodium-ion batteries can be very fast if we use a suitable electrode. The present results may form the basis for an electrode reaction for rocking chair-type sodium-ion batteries.

References

[1] D.A. Stevensa, J.R. Dahn, J. Electrochem. Soc. 147 (2000) 1271–1273.
[2] R. Alcantara, M. Jaraba, P. Lavela, J.L. Tirado, Chem. Mater. 14 (2002) 2847–2848.
[3] P. Thomas, D. Billaud, Electrochim. Acta 47 (2002) 3303–3307.
[4] R. Alcantara, J.M. Jimenez Mateos, J.L. Tirado, J. Electrochem. Soc. 149 (2002) A201–A205.
[5] R. Alcantara, P. Lavel, G.F. Ortiz, J.L. Tirado, Electrochem. Solid-State Lett. 8 (2005) A222–A225.
[6] H. Zhuo, X. Wang, A. Tang, Z. Liu, S. Gamboa, P.J. Sebastian, J. Power Sources 160 (2006) 698–703.
[7] N. Recham, J.-N. Chotard, L. Dupont, K. Djellab, M. Armand, J.-M. Tarasconz, J. Electrochem. Soc. 156 (2009) A993–A999.
[8] S. Komaba, T. Mikumo, N. Yabuuchi, A. Ogata, H. Yoshida, Y. Yamada, J. Electrochem. Soc. 157 (2010) A60–A65.
[9] L.S. Plashnitsa, E. Kobayashi, Y. Noguchi, S. Okada, J. Yamaki, J. Electrochem. Soc. 157 (2010) A536–A543.
[10] T. Abe, H. Fukuda, Y. Iriyama, Z. Ogumi, J. Electrochem. Soc. 151 (2004) A1120–A1123.

[11] T. Abe, M. Ohtsuka, F. Sagane, Y. Iriyama, Z. Ogumi, J. Electrochem. Soc. 151 (2004) A1950–A1953.
[12] T. Abe, F. Sagane, M. Ohtsuka, Y. Iriyama, Z. Ogumi, J. Electrochem. Soc. 152 (2005) A2151–A2154.
[13] F. Sagane, T. Abe, Z. Ogumi, J. Phys. Chem. C 113 (2009) 20135–20138.
[14] R.O. Fuentes, F. Figueiredo, F.M.B. Marques, J.I. Franco, Solid State Ionics 139 (2001) 309–314.
[15] F. Sagane, T. Abe, Y. Iriyama, Z. Ogumi, J. Power Sources 146 (2005) 749–752.
[16] http://www.ionotec.com/.
[17] V. Gutmann, Electrochim. Acta 26 (1976) 661–670.